

Internet Electronic Journal of **Molecular Design**

May 2006, Volume 5, Number 5, Pages 260–286

Editor: Ovidiu Ivanciuc

Special issue dedicated to Professor Lemont B. Kier on the occasion of the 75th birthday

A New Aspect in the Computational Nanomaterial Science: Odd Electrons in Molecular Chemistry, Surface Science, and Solid State Magnetism

Elena F. Sheka

Peoples Friendship University of the Russian Federation, ul. Ordjonikidze, 3, Moscow, 117198
Russia

Received: March 13, 2006; Revised: April 27, 2006; Accepted: May 1, 2006; Published: May 31, 2006

Citation of the article:

E. F. Sheka, A New Aspect in the Computational Nanomaterial Science: Odd Electrons in Molecular Chemistry, Surface Science, and Solid State Magnetism, *Internet Electron. J. Mol. Des.* 2006, 5, 260–286, <http://www.biochempress.com>.

A New Aspect in the Computational Nanomaterial Science: Odd Electrons in Molecular Chemistry, Surface Science, and Solid State Magnetism[#]

Elena F. Sheka *

Peoples Friendship University of the Russian Federation, ul. Ordjonikidze, 3, Moscow, 117198
Russia

Received: March 13, 2006; Revised: April 27, 2006; Accepted: May 1, 2006; Published: May 31, 2006

Internet Electron. J. Mol. Des. 2006, 5 (5), 260–286

Abstract

Motivation. A particular aspect of nanomaterial science concerns a common essence joining topics that seem absolutely different at first glance. This is resulted from a vital necessity to consider the main aspects of the problems at the atomic level. Thus, molecular chemistry, surface science, and solid state magnetism, their historical evolution, the language, which implies characteristic terms in use, original theoretical grounds, etc., are quite different. If radicals are widely accepted characteristics of the molecular chemistry, dangling bonds and magnetic electrons are typical terms for the surface science and magnetism. However, actually, all the features are of the same origin and are connected with *odd electrons* of atoms that form either molecules or surfaces and magnetic solids. The term stands from the difference between the number of the atom valence electrons and that one of the neighboring atoms coupled to the considered one. The current paper presents the approach application to the chemistry of fullerenes, surface science of silicon crystal as well as to the molecular magnetism of both solid polymerized fullerenes and molecular crystals composed of transitional metal complexes.

Method. The quantum theory of the electron bonding is suggested as the computational basis for the events. The study was performed computationally using the unrestricted Hartree–Fock (UHF) approximation. The AM1 semi-empirical method, implemented in the CLUSTER–Z1 program, was used for all computations.

Results. The paper concerns the molecular chemistry of fullerene, surface study of the Si(111)(7×7) and Si(100)(2×1) surfaces, molecular nanomagnets $\text{Co}_2(\mu\text{-OH}_2)(\text{OCCMe}_3)_4(\text{HOCCMe}_3)_4$ (Co_2 -molecule) and $\text{Ni}_2(\mu\text{-OH}_2)(\text{OCCMe}_3)_4(\text{HOCCMe}_3)_4$ (Ni_2 -molecule) as well as magnetism of polymerized C_{60} in view of the concept on effectively unpaired electrons.

Conclusions. The concept of effectively unpaired electrons provides a unique computational basis for description molecular chemistry of fullerenes, surface study of silicon surfaces as well as magnetic properties of molecular nanomagnets and polymerized C_{60} .

Availability. CLUSTER–Z1 software is available under request from V. A. Zayets (sheka_elena@mail.ru).

Keywords. Odd electrons; unpaired electrons; chemical activity; computational synthesis; magnetism; fullerenes; silicon surfaces; molecular magnets; magnetic polymerized C_{60} ; quantum chemistry; AM1.

[#] Dedicated on the occasion of the 75th birthday to Professor Lemont B. Kier.

* Correspondence author; E-mail: sheka@icp.ac.ru.

Abbreviations and notations

CI, configurational interaction	UHF, unrestricted Hartree–Fock
SCF, self consistent field	HF, Hartre–Fock
EUPEs, effectively unpaired electrons	RHF, restricted Hartree–Fock

1 INTRODUCTION

A peculiar aspect of nanomaterial science concerns a common essence joining topics that seem absolutely different at first glance. This is resulted form a vital necessity to consider the main aspects of the problems at the atomic level. Thus, molecular chemistry, surface science, and solid state magnetism, their historical evolution, the language, which implies characteristic terms in use, original theoretical grounds, etc. are quite different. If radicals are widely accepted characteristics of the molecular chemistry, dangling bonds and magnetic electrons are typical terms for the surface science and magnetism. However, actually, all the features are of the same origin and are connected with *odd electrons* of atoms which form either molecules or surfaces and magnetic solids. The term stands from the difference between the number of the atom valence electrons and that one of the neighboring atoms coupled to the considered one.

The very fact of the odd electron availability is absolutely necessary for the atomic system to be peculiar, while not enough. The peculiarity implementation is directly dependent on the electron behavior, mainly, on their coupling. Thus, in the case of carboneous substances such as benzene or graphite the odd electrons are fully covalently bonded and the species do not show any radical properties while siliceous aromatic molecules as well as siliceous graphite do not exist at all. The bare silicon surfaces are magnetic while the same carbon surfaces are not. Difference in the magnetic properties of the bulk traditional magnetic solids and their surfaces and/or nanosize clusters as well as different magnetic behavior of solids composed of molecular nanocomplexes of the same structure but differing by transition metals atoms (say, Ni and Co) etc. follow from the difference in coupling of the available odd electrons as well.

Historically, theoretical approaches to the phenomena have been developed in the different ways. Thus, the quantum theory of bonding forms the grounds for the molecular chemistry. At the same time, widely accepted defect–state approach to surfaces on the basis of the bulk solid state physics is mainly used in the surface science. Particular theoretical approaches concentrated on the exchange and superexchange interaction of electrons are characteristic for the solid state magnetism consideration. However, if the same origin of the events is taken into account, one can suggest a unified theoretical and/or computational approach to all the phenomena making possible their consideration on the same conceptual basis as well as on the same computational footing.

The quantum theory of the electron bonding, as the best from the atomic viewpoint, may be suggested as the computational basis for the events. However, a correct description of odd electrons necessitates taking into account the electron spins that, in its turn, requires the consideration of the

full configuration interaction (CI) in many–electron systems. As known, CI is the greatest problem of the modern quantum theory and seems to be absolutely non–feasible from the computational viewpoint when applying to nano–size objects. Any other non–full–CI approximations deal with spin–mixed electron states. Obviously, the spin–mixture of the states is bigger if the electrons are less bonded. A natural question arises if it is possible to explore the spin–mixed character of the states for the determination of the odd electrons characteristics. The answer occurs to be positive. More than 25 years ago it was suggested to use the characteristics of the spin–dependent Hartree–Fock SCF solutions for the characterization of the odd electron bonding [1]. Later on more detailed computational schemes have been elaborated [2,3]. The latest concerns the analysis of the odd electrons behavior in the frames of the advanced semi–empirical AM1 technique [4], which gives the possibility to consider versatile peculiarities of the odd electron bonding in nano–size objects on the same computational footing. The current paper presents the approach application to the chemistry of fullerenes, surface science of silicon crystal as well as to the molecular magnetism of both solid polymerized fullerenes and molecular crystals composed of transitional metal complexes.

2 THEORETICAL MODEL. ODD ELECTRONS AND THE INSTABILITY OF HARTREE–FOCK SCF SOLUTIONS

The very presence of odd electrons is fairly typical, particularly for carbon–containing molecules. These molecules are traditionally divided into two classes depending on the interaction between the electrons. If the interaction is strong, the odd electrons are entirely involved into covalent bonding accompanied by the formation of conjugated bonds (alkenes, lower aromatic and other molecules). If the interaction is weak, the electrons do not participate in covalent bonding and retain radical properties (diradicals [5,6] and carbenes [7]). A detailed investigation of the electronic structure of fullerenes C₆₀ [8–10] and C₇₀ [11] revealed a mixed character of the odd electrons pairing when one part of the electrons participates in the covalent bonding while the other forms a pool of *effectively unpaired electrons* (EUPEs below).

The study was performed computationally using the unrestricted Hartree–Fock (UHF) approximation. As is well known, the instability of a Hartree–Fock solution generally means that the energy functional $E(\Phi) = \langle \Phi | H | \Phi \rangle / \langle \Phi | \Phi \rangle$ cannot be minimized with the selected Φ_0 function. Therefore $\delta E(\Phi)|_{\Phi=\Phi_0} \neq 0$, and the problem under consideration has another solution with a lower energy. Starting since 1960, different instabilities were identified [12–18], such as spin instability (singlet and/or triplet) and instability with respect to the geometry (symmetry instability). A now–a–day analysis of the calculation results, on which the conclusions made in [12–18] were done, from the concept of odd electrons leads us to conclude that the instability of the Hartree–Fock solutions was observed for just those systems that had such electrons. As a result, researchers interested in the problem of the odd electrons behavior face the problem of selecting between two alternative

perspectives. One must either abandon the widely spread computing methods based on the Hartree–Fock approximations that do not properly include configuration interaction and wait for the development of effective computing methods including complete configuration interaction or use numerical characteristics of unstable solutions to describe the behavior of unpaired electrons. Possibilities of the first selection as well as the difficulties it involves can be estimated looking at organometallic dimer complexes considered in [19]. One of the profitable potentialities provided by following the second approach with the use of the UHF approximation was suggested in [2]. Successfully applied in the fullerene case [8–10], it seems to be enough reasonable grounds to follow this way.

The application of the Hartree–Fock approximation to systems with unpaired electrons is of general character and will be exemplified below for fullerenes which have been studied so far in more details [8–10]. As shown, the HF solutions highlighted the following distinguishing features:

(1) The $E_{S=0}^{RHF}$ and $E_{S=0}^{UHF}$ singlet state energies calculated in the RHF (closed shell) and UHF (open shell) approximations, respectively, do not coincide. Their difference $E_{rad} = E_{S=0}^{RHF} - E_{S=0}^{UHF}$ reveals the molecule radicalization and can be called the *radicalization energy*.

(2) According to the UHF solution, the spin density on the atoms $D_A^{(1)}$ in the singlet state is nonzero ($D_A^{(1)}$ is determined as $D_A^{(1)} = \sum_{i \in A} P_{ii}^{(1)\alpha} - P_{ii}^{(1)\beta}$, where P_{ii}^α and P_{ii}^β are the density matrix elements for the electrons with spins α and β , respectively). This results from the exclusion of odd electrons from the covalent pairing.

(3) The eigenvalue $\langle S^2 \rangle^{(1)}$ of the \hat{S}^2 operator is nonzero. The result evidences that the UHF wave function of the singlet state is not eigenfunction of the operator \hat{S}^2 .

Nonzero radicalization energy evidences that the RHF solution is unstable. However, the UHF solution, which is spin–mixed because $\langle S^2 \rangle^{(1)} \neq 0$, is also unstable, since, according to [2], the molecule has a pure spin state with a lower energy $E_{S=0}^{PS}$ that is determined as $E_{S=0}^{PS} = E_{S=0}^{UHF} + S_{max} J$, where the exchange interaction integral J is given by

$$J = \frac{E_{S=0}^{UHF} - E_{S=S_{max}}^{UHF}}{S_{max}^2} \quad (1)$$

and $S_{max} = n$ is the maximum spin of n electron pairs [2]. Here $E_{S=0}^{UHF}$ and $E_{S=S_{max}}^{UHF}$ are spin–mixed singlet state and spin pure state with the highest multiplicity, respectively. The pure spin states are lowest in energy if J is negative, that corresponds to the antiferromagnetic coupling of spins. For this reason, it is these states that should be considered the ground states, which is evidence of the singlet instability of both RHF and UHF solutions. Thus, the problem arises of obtaining the main characteristics (energy, structure, and wave function) of the system in the pure spin singlet states.

This causes necessity to estimate the degree of accuracy of using the UHF solution as a reasonable approximation to the pure spin state. Quantitative estimations are exemplified by the case of the C₆₀ molecule.

2.1 Wave Function

As is well known, the one-determinant singlet wave function T_0 (see the notation in [15]), which is the eigenfunction of the UHF Hamiltonian of the system of n pairs of electrons, is generally not the eigenfunction of the squared spin operator \hat{S}^2 . It is this circumstance that is responsible for nonzero $\langle S^2 \rangle^{(1)}$ values obtained in the UHF calculations of the singlet state of fullerene molecules. Applying the projection operator, one can extract the pure spin singlet state function from the T_0 function. According to [15], the pure spin function has the form

$$\Psi^{(1)=^{(1)}\Theta} T_0 = c_0^{(0)} \sum_{k=0}^n (-1)^k \binom{n}{k} T_k, \quad (2)$$

where the index k is the number of permuted electrons and the T_k functions are the sets of determinants that can be written as [15]:

$$\begin{aligned} T_0 &= (N!)^{-1/2} \det \langle a_1 \alpha a_2 \alpha \dots a_n \alpha | b_1 \beta b_2 \beta \dots b_n \beta \rangle \\ &= \langle \alpha \alpha \alpha \dots \alpha | \beta \beta \beta \dots \beta \rangle \\ T_1 &= \langle (\beta \alpha \alpha \dots) + (\alpha \beta \alpha \dots) + \dots | (\alpha \beta \beta \dots) + (\beta \alpha \beta \dots) + \dots \rangle \\ T_2 &= \langle (\beta \beta \alpha \dots) + (\beta \alpha \beta \dots) + \dots | (\alpha \alpha \beta \dots) + (\alpha \beta \alpha \dots) + \dots \rangle \\ &\dots\dots\dots \\ T_n &= \langle \beta \beta \beta \dots \beta | \alpha \alpha \alpha \dots \alpha \rangle \\ T_{-1} &= T_{n+1} = 0. \end{aligned} \quad (3)$$

The right-hand side of Eq. (2) is an alternating series; it can be represented in the form

$$\Psi^{(1)} = c_0^{(0)} \left\{ [T_0 + (-1)^n T_n] - \frac{1}{n} [T_1 - (-1)^{n-1} T_{n-1}] + \frac{2}{n(n-1)} [T_2 + (-1)^{n-2} T_{n-2}] - \dots + (-1)^{n/2} \frac{(n/2)!(n/2)!}{n!} T_{n/2} \right\}. \quad (4)$$

Here, $n = N/2$, where N is the total number of electrons while T_0 and T_n are the one-determinant UHF functions. If n is even, (4) begins with the term $T_0 + T_n$ and contains terms with even numbers only. Because the T_1 and T_{n-1} functions are equal according to (3), the odd terms disappear. The series ends by the term with the number $n/2$. If n is odd, the terms with even numbers are excluded from (4). This series then begins with the term $T_1 + T_{n-1}$ and ends by the term with the number $(n+1)/2$. If n is large, the contribution of the terms starting with the second is small in both cases (for instance, with fullerene C₆₀, the contribution value is $\sim 10^{-4}$). It follows that the wave function of the pure spin singlet state can be written to a good approximation as

$$\begin{aligned}\Psi^{(1)} &\approx c_0^{(0)}[T_0 + T_n], \text{ if } n \text{ is large and even,} \\ \Psi^{(1)} &\approx -\frac{c_0^{(0)}}{n}[T_1 + T_{n-1}], \text{ if } n \text{ is large and odd.}\end{aligned}\quad (5)$$

In the first case, the $\Psi^{(1)}$ wave function is an UHF function. In the second case, the detailed form of $\Psi^{(1)}$ is difficult to analyze. In the problem of the electronic properties of the fullerene molecule, we deal with functions of the first type. The results of the UHF solution based on the properties of its wave function can therefore be transferred to the pure spin singlet state.

2.2 System Energy

The relative change in the energy in going from the UHF to pure spin singlet state is [15]:

$$\frac{\Delta E^{(1)}}{E_{UHF}^{(1)}} = -\frac{1}{n} \left\{ \int T_0^* H T_1(dx) / \int T_0^* H T_0(dx) \right\} \quad (6)$$

It equals ~6% and 2% for C₆₀ and Si₆₀ ($n = 120$), respectively, and ~6% for C₇₀ ($n = 140$) (see Table 2). These values estimate the accuracy of replacing the pure spin state by the UHF solution with respect to the energy. This accuracy proves to be not too low.

2.3 Molecular Structure

This problem is thoroughly discussed in [12–18] from the viewpoint of the influence of the energy lowering on the structure. It is commonly believed that energy lowering is accompanied by a descent of symmetry (this adds geometry and/or symmetry instability to the spin instability). A comparison of the equilibrium structure obtained using an UHF solution with experimental data can then be used as a criterion of the acceptability of this solution. Fullerene C₆₀ highlights the situation particularly clear that will be discussed in Section 3.

2.4 The Spin Characteristics of the System of Odd Electrons

Let us return to the spin characteristics of the system of the odd electrons in terms of the UHF solution. As has been mentioned above, these include a nonzero spin density on the atoms $D_A^{(1)}$ and a nonzero $\langle S^2 \rangle^{(1)}$ value. The appearance of both is caused by the above-mentioned EUPEs, which were firstly considered more than 25 years ago [1]. As shown, the EUPEs distribution can be described by the density function

$$D(r|r') = 2\rho(r|r') - \int \rho(r|r'')\rho(r''|r')dr'' \quad (7)$$

In the UHF approximation, the $D(r|r')$ has the form

$$DS = 2PS - (PS)^2, \quad (8)$$

where $P = P^\alpha + P^\beta$ is the density matrix and S is the orbital overlap matrix. In the *NDDO* approximation that is implemented in the computational tool in use below, a nonzero overlap of

orbitals results in $S = I$, where I is the identity matrix. The density matrix D then takes the form [4]

$$D = (P^\alpha - P^\beta)^2. \quad (9)$$

The elements of the density matrices $P_{ij}^{\alpha(\beta)}$ can be written in terms of the eigenvectors of the UHF solution as

$$P_{ij}^{\alpha(\beta)} = \sum_k^{N^{\alpha(\beta)}} C_{ik}^{\alpha(\beta)} * C_{jk}^{\alpha(\beta)}. \quad (10)$$

where N^α and N^β are the numbers of the electrons with spins α and β , respectively. As shown [4], the EUPES number on atom A can be calculated as

$$N_{DA} = \sum_{i \in A} \sum_{B=1}^{NAT} \sum_{j \in B} D_{ij}. \quad (11)$$

while the total EUPES number $N_D = \sum_A N_{DA}$ is determined as a summation over all orbitals:

$$N_D = \sum_{i,j=1}^{NORBS} D_{ij}, \quad (12)$$

A nonzero squared spin value in the singlet state is evidence of the EUPES presence as well. According to [3], the EUPES total number is given by the equation

$$N_D = 2 \left(\langle S^2 \rangle - \frac{(N^\alpha - N^\beta)^2}{2} \right) \quad (13)$$

where, according to [20],

$$\langle S^2 \rangle = \frac{(N^\alpha - N^\beta)^2}{4} + \frac{N^\alpha + N^\beta}{2} - \sum_{i,j=1}^{NORBS} P_{ij}^\alpha * P_{ij}^\beta. \quad (14)$$

Equations (11)–(14) were used in the calculations presented in this work. The AM1 semi-empirical method, implemented in the CLUSTER-Z1 program [21], lays the calculation foundation. The program provides stable UHF calculations in singlet states supplemented by the calculations of all above-mentioned quantitative characteristics related to unpaired electrons [4].

3 DIATOMIC MOLECULES

Analyzing the behavior of the N_D values along the potential energy curve of a diatomic molecule forms an excellent possibility for checking the correctness of the UHF solutions. The calculations were performed for the hydrogen, nitrogen, and oxygen molecules (calculation details are given in [4]). The calculation data for the ground state of the molecules (singlet for H_2 and N_2 , and triplet for O_2) are shown in Figure 1. The first result is the coincidence of the N_D values calculated independently using (11) and (12). Next, the character of the $N_D(R)$ dependencies was common to

all molecules. Each $N_D(R)$ curve contains three regions, namely, $R \leq R_{cov}$ (I), $R_{cov} < R \leq R_{rad}$ (II) and $R > R_{rad}$ (III) (the R_{cov} and R_{rad} values for the oxygen molecule are shown in Figure 1). The R_{cov} distance corresponds to complete covalent bonding of the molecule electrons according to the multiplicity of its ground state, and R_{rad} , to the separation of the molecule atoms sufficient for the formation of two free radicals. It should be noted that region II is rather narrow. The difference $R_{rad} - R_{cov}$ fills the region of 1–1.5 Å in width.

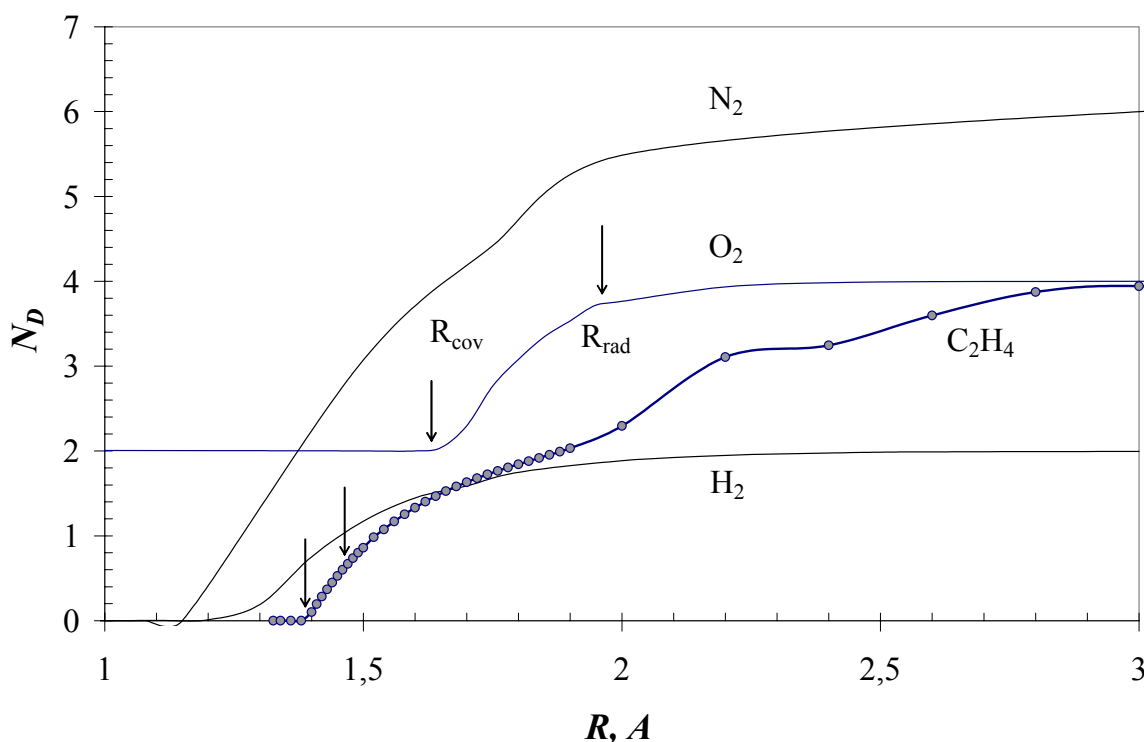


Figure 1. The number of effectively unpaired electrons N_D in diatomic molecules and ethylene as a function of the distance between nuclei.

Let us consider the main features of the $N_D(R)$ dependencies for the hydrogen and nitrogen molecules. The ground state of both is singlet, and for this state both curves were calculated. As expected, there are no unpaired electrons in region I. As a consequence, the UHF and RHF solutions coincide and are stable. The number of unpaired electrons in region III must be 2 and 6 for hydrogen and nitrogen, respectively. According to Figure 1, the $N_D(R)$ curves do indeed approach the asymptotes corresponding to 2 and 6 electrons in this region. The nonzero N_D values obtained in our calculations of the singlet state evidence the obvious singlet instability of the UHF solution in this region. The calculations nevertheless correctly reproduce the physically expected numbers of unpaired electrons. In the transition region II, the number of unpaired electrons cannot be substantiated by independent physical arguments. The degree of the solution instability can be estimated from the dependence of the solution on the starting density matrix. With hydrogen and nitrogen, this dependence is weak. This leads us to conclude that the dependencies shown in Figure 2 correspond to physical reality. With oxygen, the analysis of the results obtained in regions I and

III shows a similar behavior.

In view of carbeneous species, the most interesting is the C₂ pair. However, C₂ pairs differ by the number of odd electrons, which constitutes 6 for the C₂ dimer, 4 for acetylene C₂H₂ and 2 for ethylene C₂H₄. The latter would be the most appropriate for aromatic compounds, graphite, fullerenes, carbeneous nanotubes. The evolution of the total number of unpaired electrons along the potential curve for the ethylene molecule is shown in Figure 1 by a curve with dots. After calculating the equilibrium structure with the C–C bond of 1.326 Å in length, the C–C distance was kept fixed at a preset value at every next step of calculations while the hydrogen atom positions were optimized.

Table 1. Effectively unpaired electrons in aromatic molecules, UHF singlet state

Molecules	C–C bond length, Å				N _D
	Number of bonds				
Benzene	1.395 6				0
Naththalene	1.385 4	1.411 2	1.420 4	1.430 1	1.483
Anthracene	1.387 4	1.410 6	1.421 4	1.435 2	3.003
Tetracene	1.388 4	1.410 8	1.421 6	1.436 3	4.320
Pentacene	1.388 4	1.411 10	1.420 8	1.436 4	5.540

As seen from the figure, the $N_D(R)$ behavior is similar to that one of the diatomic molecules discussed above. As previously, region I corresponds to covalently bound electrons with $N_D = 0$ until R reaches R_{cov} equal to 1.395 Å. On the other side, when R reaches R_{rad} equal to 3.00 Å, N_D approaches 4 showing a total radicalization of the CH₂-CH₂ pair. The interval between 1.395 Å and 3.00 Å corresponds to the intermediate case when the odd electrons change their behavior from totally bonded to radical free. Therefore, the state of the electron pair depends on the atom distance so that the greater is the number of long C–C bonds, the bigger EUPE total number should be characteristic for a molecule. Let us check this point for $2n$ -aromatic molecules. As seen from Table 1, the molecules have practically the same set of the C–C bonds while differing in the related bond number, particularly with respect to long bonds. The N_D values presented in the table show that increasing the number of long bonds in the molecules is followed by increasing the N_D values indeed. One can conclude from this that just the availability of long bonds in fullerenes causes their odd electron unpairing. Two arrows attached to the ethylene curve in Figure 1 marks the bond length interval characteristic for fullerenes. As seen, the interval is located in the intermediate region above R_{cov} . It is important that within the UHF approach $R_{cov} = 1.395$ Å is an extreme point above which electron unpairing occurs. In graphite, graphene, carbeneous nanotubes the bond lengths exceed the limit value that causes an effective odd electron unpairing in these structures [22]. As seen from Table 1, the molecules have practically the same set of the C–C bonds while

differing in the related bond number. The N_{Dadd} values are obtained by summing the N_D quantities at the corresponding C–C bond length from the data obtained above for ethylene. The N_D values presented in the table are obtained by direct calculations. The data show that the additivity does really take place in the case with the accuracy of $\sim 20\%$ for naphthalene while with much higher accuracy for larger molecules. Obviously, increasing the number of long bonds in the molecules is followed by increasing the N_D values.

Surely, it should not be a global law and if the aromatic molecule flatness is undoubtedly favorable for the additivity, the 3D complex structure of fullerenes does not favor the law and $N_{Dadd} > N_D$ in the case. Nevertheless, just the availability of long bonds in the molecules is responsible for the odd electron unpairing. Two arrows attached to the ethylene curve in Figure 1 shows the bond length interval characteristic for fullerenes. It is important that $R_{cov} = 1.395 \text{ \AA}$ is a limit point above which electron unpairing occurs. In graphite, graphene, carbonaceous nanotubes the bond lengths exceed the limit value that causes an effective odd electron unpairing in these structures [22].

4 MOLECULAR CHEMISTRY OF FULLERENE

4.1 Molecular Structure

Gas phase electron diffraction of the C_{60} molecule tells us that the molecule shape is a truncated icosahedron which is formed by two types of the C–C bonds, ones of a substantial double bond character and of $h = 1.398(10) \text{ \AA}$ in length while the other are of $p = 1.455(6) \text{ \AA}$ long and have a prevalent single bond character [23]. 60 carbon atoms are arranged in 20 six-membered and 12 five-membered rings. The C–C bonds separating two hexagons are double bonds (h) while the pentagon C–C bonds (p) are single. Supposing all C–C bond lengths to be of the same length within the group, the molecule configuration was attributed to the icosahedral (I_h) symmetry group. Later on close shell calculations of the molecule equilibrium configuration supported this conclusion. As shown earlier, the relevant solutions are unstable. What is going on when we pass to the open shell approximation which is in better accordance with the pure spin singlet state? As occurred, the UHF solution supports the molecule icosahedron shape formed by two groups of the C–C bonds, but shows lower C_i symmetry of the structure due to considerable scattering the bond length that is shown in Figure 2. The very fact is fully consistent with general regulations discussed in [12–18] but a discrepancy with the experimental data could be seen. However, the discrepancy is an illusion. As seen from the figure, the symmetry lowering is caused by the length dispersion increasing when going from the RHF to UHF solution and the two symmetry-different structures can be distinguished if only the accuracy of the bond length determination is better than 10^{-2} \AA . Evidently, the accuracy of the diffraction experiment [23,24] is close to the limit, so that the conclusion about the I_h symmetry of the molecule is based on fixed *average* lengths. Precise determination of the molecular geometry by neutron scattering from the C_{60} powder [25] gives values $h = 1.391 \pm 0.063 \text{ \AA}$

and $p = 1.452 \pm 0.066 \text{ \AA}$ that are even less accurate from the experimental viewpoint and are well consistent with the UHF data. The same can be addressed to the X-Ray data for the C_{60} crystal [26]. Therefore, structural experiments are not discriminative for the case, indeed. Oppositely, an exhausted and detailed analysis of highly structure-sensitive electronic optical spectra of C_{60} forced the authors to conclude that the molecule symmetry is evidently not I_h , but substantially lower [27]. Similar conclusion can be made from the analysis of the molecule Raman spectra, revealing symmetry “silent” modes as well as splitting of all degenerated bands [28]. Both features show convincingly the molecule symmetry lower than I_h .

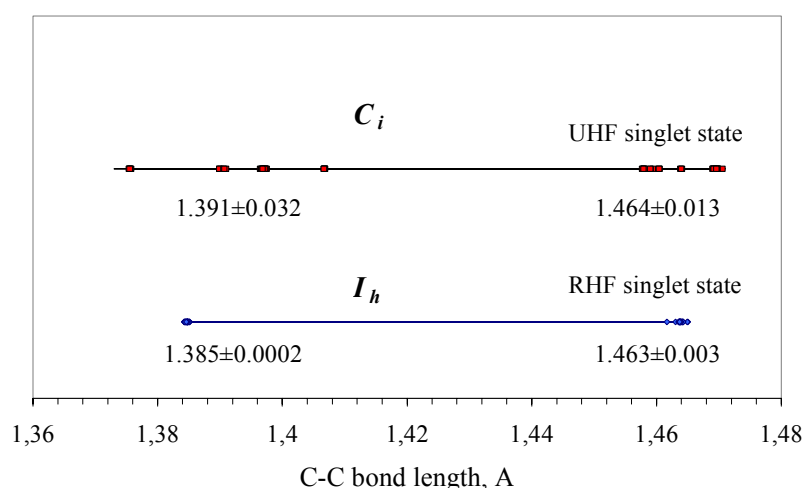


Figure 2. Dispersion of the C–C bonds of the C_{60} molecule.

The UHF solution, similarly to the RHF one, supports the difference in the character of the bonds. Thus, the short bonds have close to the double bond character, which might be characterized by the Wiberg bond index [28]. In both cases the average Wiberg index for the bonds is 1.494 but with different dispersion of ± 0.0005 and ± 0.08 for the RHF and UHF solutions, respectively. As for the long bonds, the average Wiberg index of 1.10 clearly evidences the single bond character with the corresponding dispersions of ± 0.001 and ± 0.03 .

4.2 Effectively Unpaired Electrons and Free Valence of Fullerene Molecules

The EUPEs total number N_D in the C_{60} and C_{70} molecules is 9.84 and 14.4, respectively, or approximately 20% of the total number of odd electrons. For Si_{60} $N_D = 63.4$, that is, all the 60 odd electrons are unpaired. These results quantitatively confirm partial radicalization of the C_{60} and C_{70} molecules while a complete radicalization of Si_{60} takes place. This, in particular, explains the impossibility of producing the latter substance. The distribution of N_D over the atoms of Si_{60} and C_{60} according to (11) is shown in Figure 3. In complete agreement with the above reasoning, the N_{DA} values are close to one for the majority of Si_{60} atoms, whereas those for C_{60} do not exceed ~ 0.3 . The picture obtained for C_{70} was similar to that for C_{60} . It is natural to compare the N_{DA} values with the free valence of atoms. The free valence distributions over the atoms of the molecules are shown

by solid lines in Figure 3. The quantity is defined as

$$V_A^{free} = N_{val}^A - \sum_{B \neq A} K_{AB} \quad (15)$$

where N_{val}^A is the number of valence electrons of the A atom and $\sum_{B \neq A} K_{AB}$ is the generalized bond index, $K_{AB} = |P_{AB}|^2 + |Sp_{AB}|^2$. Here, the first term is the Wiberg bond index [29] and the second term is determined by the spin density matrix (see [30] for details). Excellent agreement of the two values shows that the N_{DA} value can be used as a quantitative measure of the free valence or chemical activity of atoms and as a pointer of the atom–atom contacts which should be most active in addition reactions. This opens a possibility of a large *computational synthesis* of any fullerene–based derivative just selecting the fullerene core target atoms by the largest N_{DA} value.

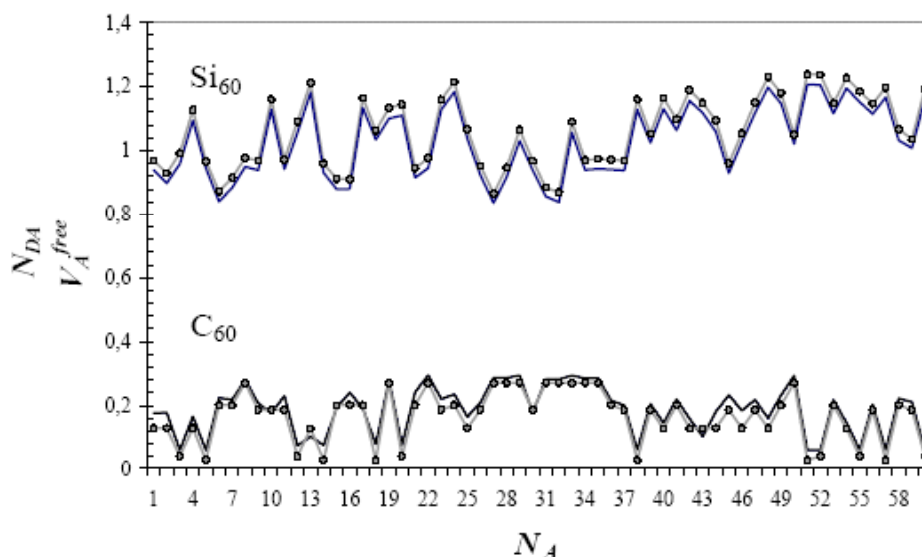


Figure 3. Distributions of N_{DA} (open circles) and free valence (solid lines) over the atoms in C_{60} and Si_{60} [4].

4.3 Chemical Portraits of Fullerene Molecules

Let us consider the N_{DA} maps of the C_{60} and C_{70} fullerenes more attentively.

4.3.1 C_{60} fullerene

The EUPES density is distributed over the molecule atoms as shown in Figure 4. The N_{DA} map in Figure 4a corresponds to numbering of atoms from the input/output files (as was in Figure 3). The figure shows that the value varies in a rather wide region from zero to 0.32. However, if the N_{DA} values are aligned by the value lowering, the distribution takes more ordered view as seen in Figure 4b. The map clearly shows five groups with 12 atoms in each, which are characterized by the same N_{DA} value. Atoms of each group form six identical pairs consisted of two carbon atoms coupled via a short C–C bond. Spin densities on the two atoms in any pair are equal by values and differ by sign.

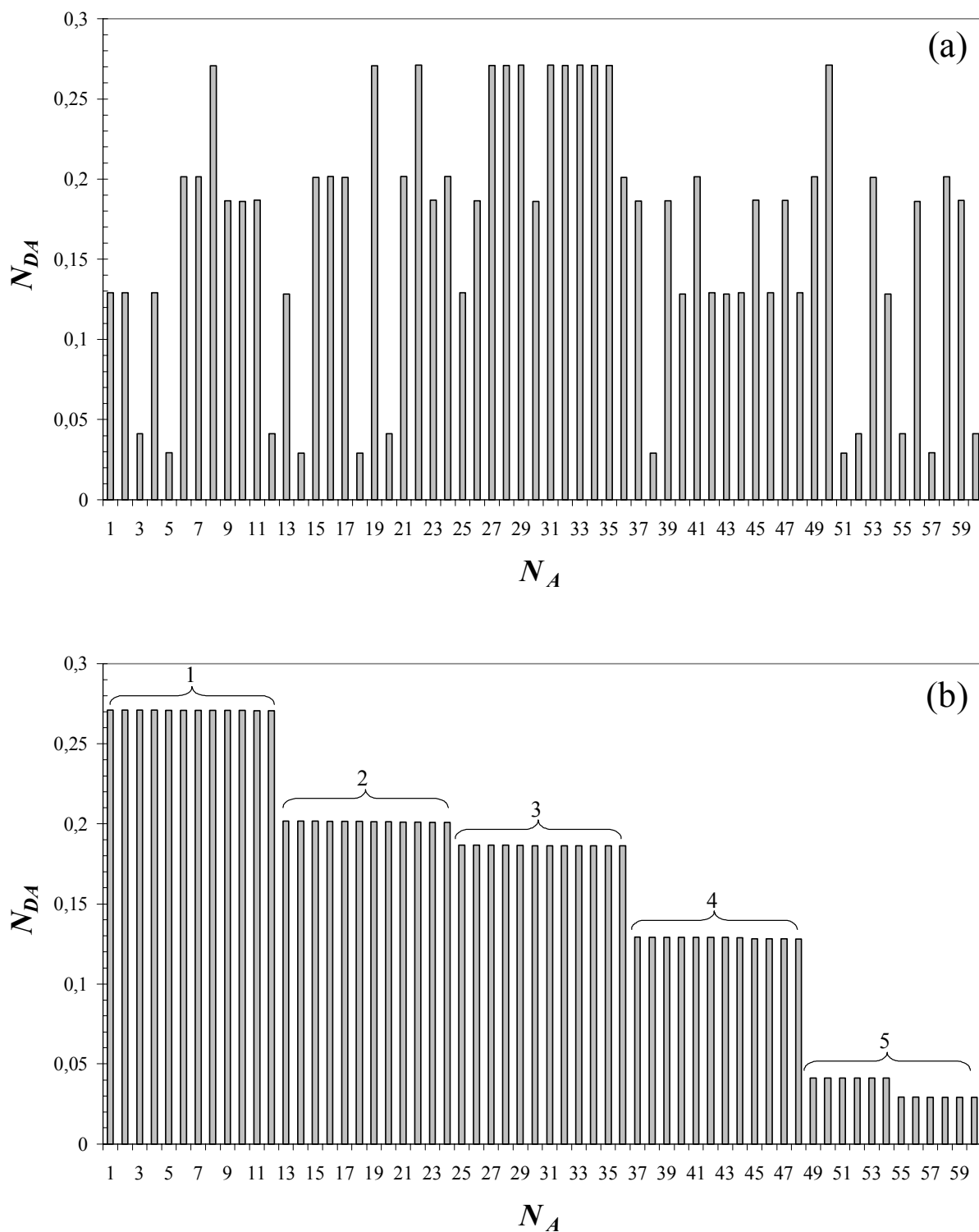


Figure 4. The N_{DA} map of C_{60} [33].

Therefore, the C_{60} molecule consists of six identical C_{10} compositions formed by five pairs in accordance with the total number of the groups. Distributing atoms over six fragments following the N_{DA} map shown in Figure 4a, one gets a $6 \cdot C_{10}$ configuration consisting of six identical naphthalene cores shown in Figure 5a. Applying different coloring to atoms of different N_{DA} values, one obtains a *chemical portrait* of the C_{60} molecule in the singlet UHF state. The picture unexpectedly favors a

hypothesis of the C_{60} molecule formation from mutually bonded carbene chains C_5 suggested ten years ago [31] and later actively discussed [32].



Figure 5. The “chemical portrait” of C_{60} [30].

The contrast of the N_{DA} map, or the gradient of the atom chemical activity, is determined by the difference of the N_{DA} values of the atoms belonging to different groups. That forms the grounds for the atomic–local selectivity of the molecule chemical activity. Thus, any atom of group 1 from two hexagons at antipodal ends of the molecule (see Figure 5b) are undoubtedly preferable for initial steps of addition reactions.

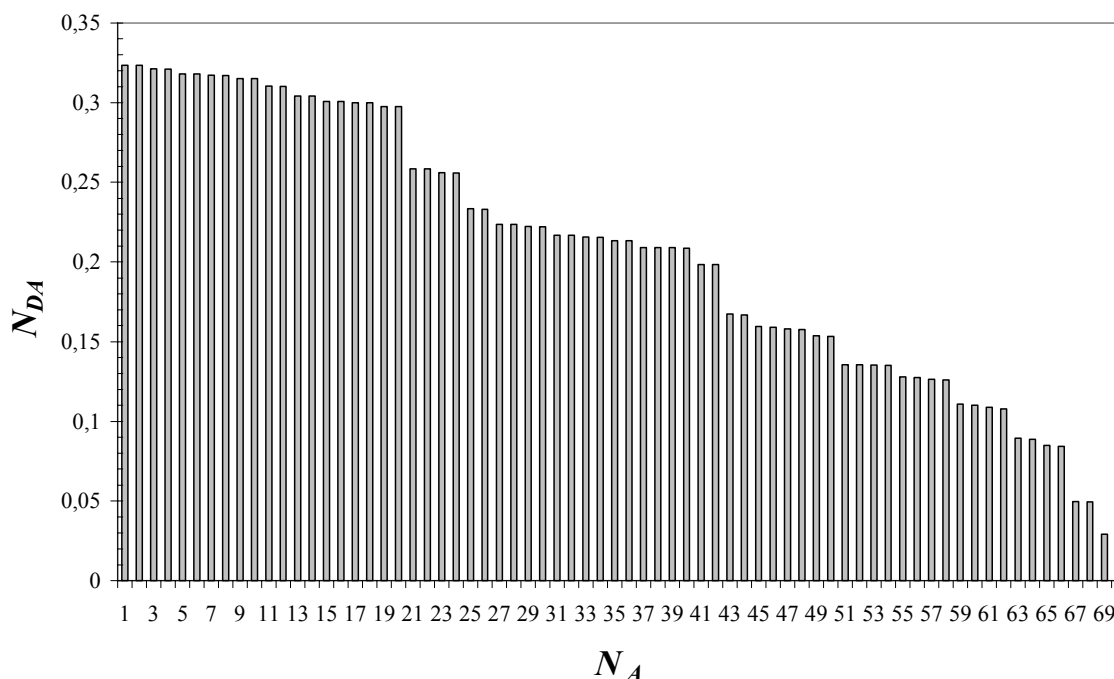


Figure 6. The N_{DA} map of C_{70} .

4.3.2 C_{70} fullerene

The N_{DA} map of the molecule shown in Figure 6 evidences much less contrast in comparison with that of C_{60} . Nevertheless, as previously, the N_{DA} distribution shows well–defined grouping. Oppositely to the previous case, we cannot distinguish a unique basic structural element, multiplying which one can compose the molecule structure. The D_{5h} symmetry of the molecule in

the UHF singlet state (see Figure 7a) suggests the molecule structure decomposition into three five-membered circular fragments shown in Figures 7b and 7c. Hexagon C_6 is the common element of the fragments. Those are conjugated in two 20-atom fragments **I** in Figure 7b, forming figures of five-lobe flowers. Five hexagons of fragment **II** in Figure 7c form a 30-atom closed rarefied chain-bracelet mutually coupled via a single C–C bond. The maximum N_{DA} values are concentrated in the circular belt-bracelet **II**. Therefore, the area unites atoms with the highest initial chemical activity.

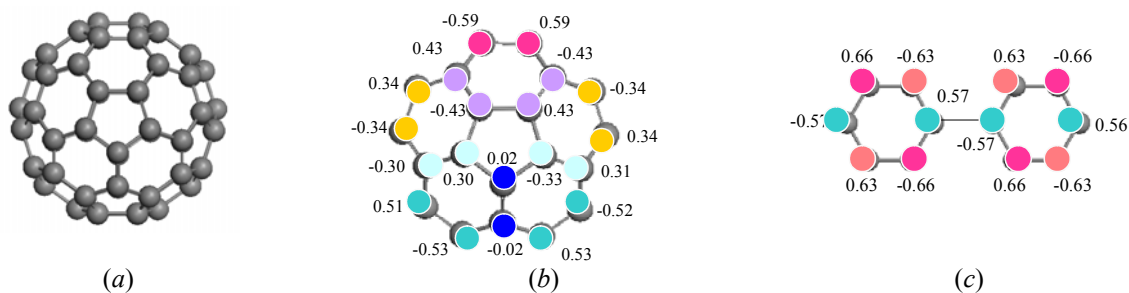


Figure 7. The “chemical portrait” of C_{70} . Figures show spin density on atoms.

4.4 Basis for the Computational Synthesis of the C_{60} Fullerene Derivatives. Synthesis of Fluorinated Fullerenes.

Suggesting the N_{DA} value as a quantitative indicator of the atom chemical activity, let us proceed to a computational synthesis of the C_{60} molecule derivatives on the basis of the N_{DA} map. A well studied reaction of the C_{60} fluorination in the gaseous state [34,35] has been taken as an example. Starting calculations, we chose a pair of atoms with the biggest N_{DA} values from one of six naphthalene-core fragment (see cross-marked atoms on the initial map in Figure 8). A fluorine molecule is placed in the vicinity of the atoms (see Figure 9a) and a full optimization of the complex geometry in the singlet state is performed. As occurred, the fluorine molecule is willingly attached to the fullerene, however, two adducts are possible depending on the fluorine molecule orientation with respect to the chosen C–C bond. If the molecule axe is parallel to the bond, the adduct $C_{60}F_2$ (**I**, Figure 9b) is formed. If the molecule axe is inclined towards the bond, even so slightly as shown in Figure 9a, a complex $C_{60}F_1 + F_1$ (**II** + F_1 , Figure 9c) is obtained.

The N_{DA} maps for the fullerene core of adducts **I** and **II** are shown in Figure 8. The relevant map of a free fullerene molecule forms background in both figures. Crosses mark initial target carbon atoms (31 and 32 in the case). As seen from the figure, attaching either one or two fluorine atoms changes the initial map considerably and differently in both cases. When two atoms are attached to the core (Figure 10b), the N_{DA} values become zero for target atoms 31 and 32 and star-marked atoms 18, 20, 38 and 55 become the most active.

When one atom is attached, remaining target atom 31, which is adjacent to the first target atom 32, dominates on the adduct map (Figure 8b). The picture clearly evidences a readiness of the C_{60} core to complete the reaction by adding another fluorine atom to atom 31. Following this indication,

and keeping configuration of the **II**+F complex, we add one more fluorine molecule, as shown in Figure 9d. In due course of the structure optimization, a new adduct $C_{60}F_2 + 2F$ (**III**+2F, Figure 9e) is formed. Geometry and electronic properties of adduct **III** are fully identical to those of adduct **I** that is confirmed by a complete identity of their N_{DA} maps as well. Therefore, independently of either one-stage (Figure 9b), or two-stage (Figure 9e) processes of the fluorine attachment to the fullerene core occur, the same final adduct $C_{60}F_2$ is formed. Obviously, two-stage reaction should prevail in practice.

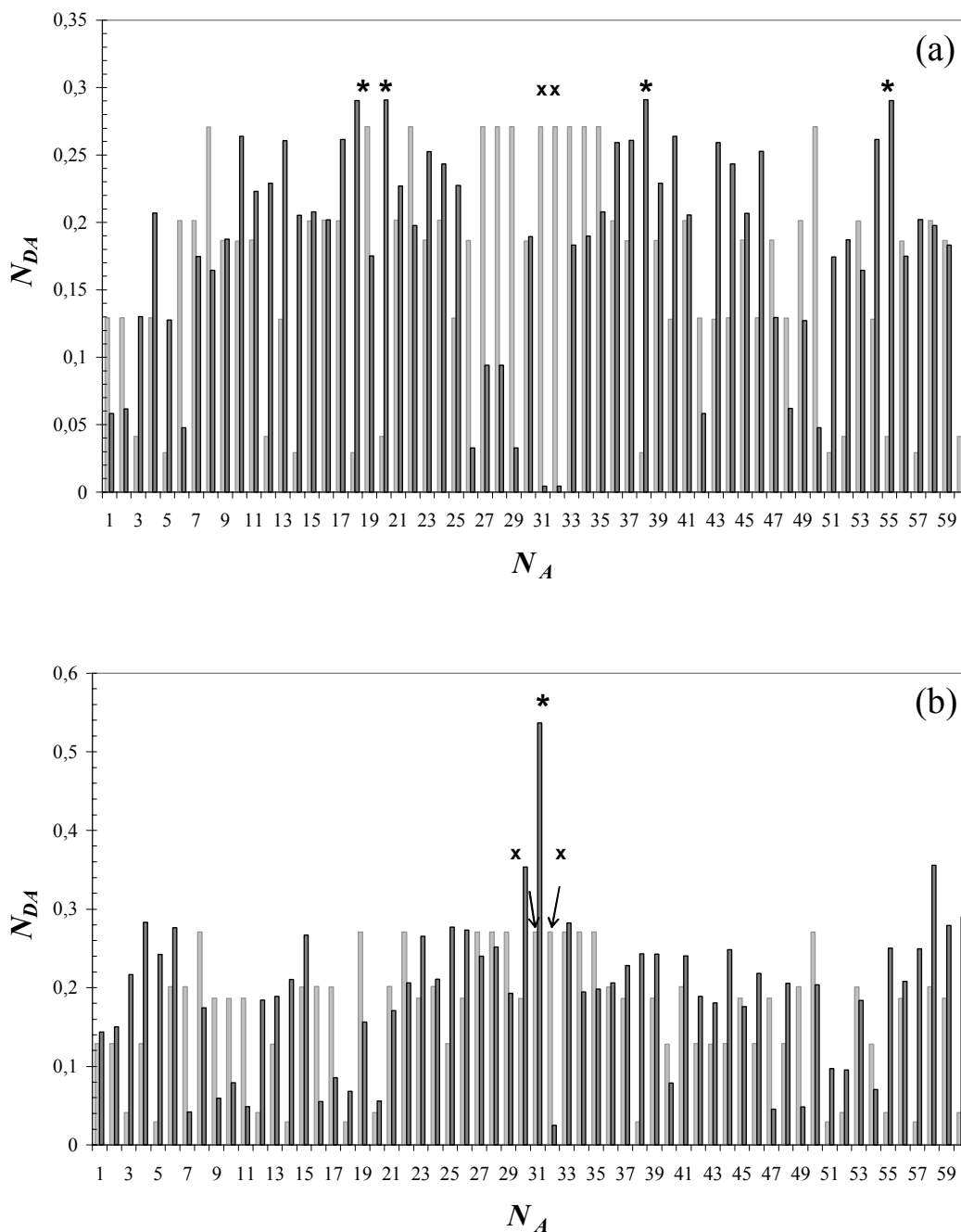


Figure 8. N_{DA} map of the C_{60} core of adducts $C_{60}F_2$ (a) and $C_{60}F_1$ (b). Light-color bars present the map of a free C_{60} molecule.

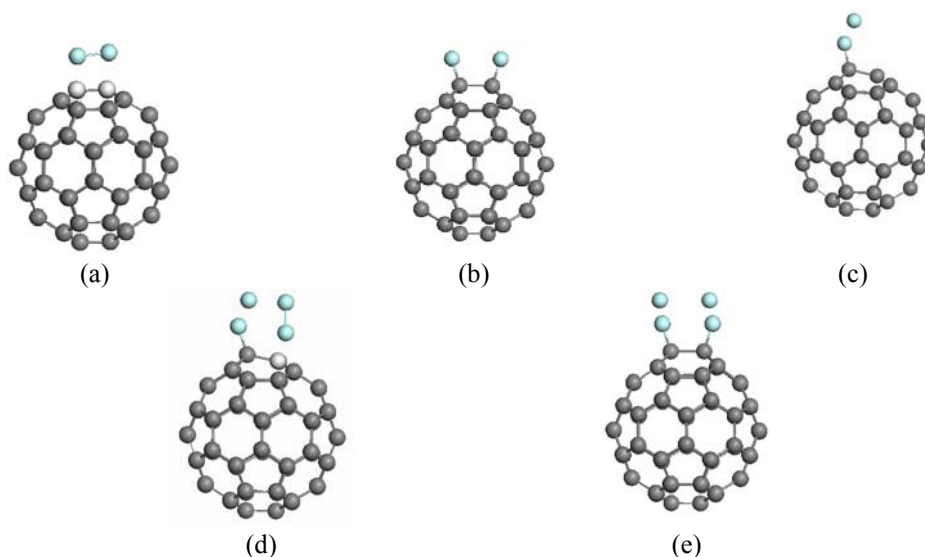


Figure 9. Attaching of a fluorine molecule to the C_{60} core. *a.* Starting geometry. Target atoms of the C_{60} core are shown by light coloring. *b.* Adduct I $C_{60}F_2$ *c.* Adduct II $C_{60}F_1$ and a free fluorine atom F_1 ; the composition corresponds to the starting geometry in *a.* Starting configuration (*d*) and final adduct (*e*) of the reaction $(C_{60}F_1 + F_1) + F_2$. Target atom of the C_{60} core is shown by light coloring.



Figure 10. Attaching of a fluorine molecule to the $C_{60}F_2$ core. *a.* Starting geometry. Target atoms of the C_{60} core are shown by light coloring. *b.* Adduct $C_{60}F_4$.

The next step of the reaction is governed by the predominance of atoms 18, 20, 38 and 55 on the N_{DA} map of the $C_{60}F_2$ molecule (see Figure 8a). The atoms form two equivalent pairs of short C–C bonds located in the equatorial plane with respect to first two target atoms (see light colored atoms in Figure 10a). One of these pairs is taken as targeting and the procedure of attaching fluorine atoms to the pair atoms repeats the described above. Consequently, a molecule $C_{60}F_4$ is formed (Figure 10b). The N_{DA} map is calculated for the product to select target atoms for the next attaching. Since, as shown, two-stage process of the F_2 addition should be more common, the computational synthesis of fluorinated fullerenes $C_{60}F_{2n}$ has been performed [52] as a series of subsequent steps, consisting of two stages which involved calculations of two adducts related to two reactions $C_{60}F_{2k} + F_2 = C_{60}F_{2k+1} + F$ and $C_{60}F_{2k+1} + F_2 = C_{60}F_{2(k+1)} + F$, $k = 1, 2, \dots, 30$. Each step is controlled by the fullerene core N_{DA} map of the preceding adducts, namely, $C_{60}X_{2k}$ and $C_{60}F_{2k+1}$, respectively. Actually, every step is additionally complicated by expanding calculations over a set of isomers which are pointed out by a set of high-rank values on the N_{DA} map. A choice of the most stable species is subordinated therewith to the preference of the structure with the least energy. Practically,

the computational procedure involved from two to eight isomers at every computational step [36]. The validity of the synthesis performed is supported by good fitting of the calculated and experimentally known structures. Thus calculated species $C_{60}F_{18}$, which is energetically the most stable, has C_{3v} symmetry with fluorine atoms bounded to one hemisphere of the C_{60} cage in full accordance with experimental data [37]. The structure of the $C_{60}F_{48}$ species fits perfectly well the recent precise X-ray data [38]. Detailed description of the family synthesis is given elsewhere [36].

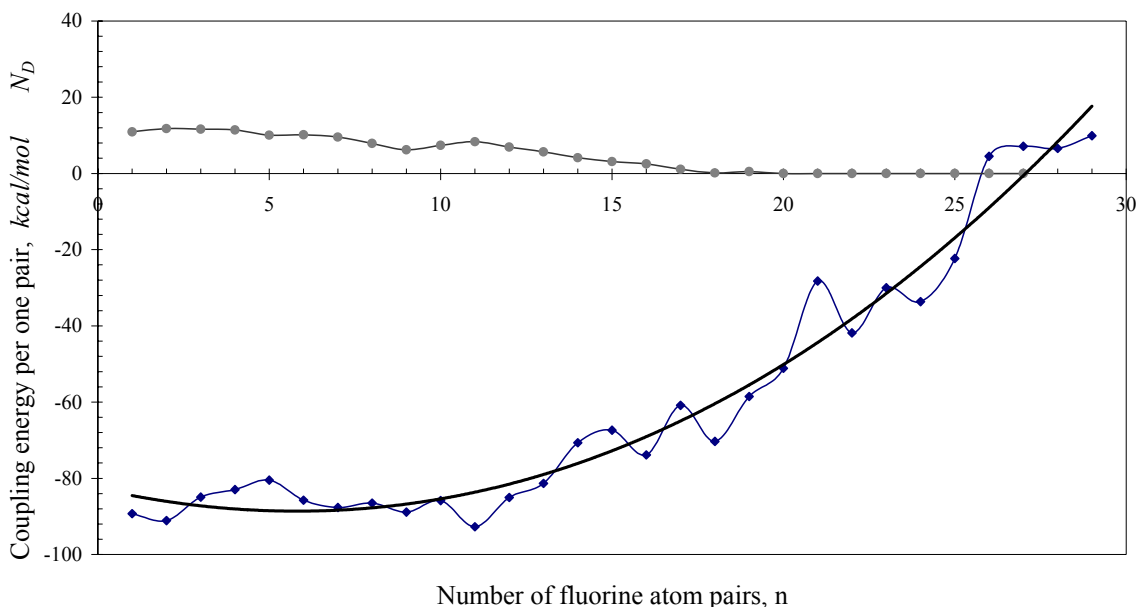


Figure 11. Evolution of the N_D value and the coupling energy with the number of fluorine atom pairs [36].

Figure 11 presents the coupling energy which accompanies every new act of two fluorine atoms addition. Changing in the N_D value is shown in the upper part of the figure. As seen, the coupling energy is rather irregular within the series indicating a preference towards particular molecular compositions related to $k = 2, 9, 11, 16, 18, 22, 24$. However, in general, the energy gradually decreases when k increases and the value becomes positive when k exceeds 25. On the other hand, the N_D value decreases when fluorinations proceeds indicating that the chemical activity pool is gradually worked out, so that N_D approaches zero at $k = 22$. Both tendencies illustrated in Figure 11 show that the fluorination of fullerene C_{60} by gaseous fluorine should stop at $k = 24$ that well correlates with experimental findings [37].

A similar synthesis has been performed for C_{60} hydrated and aminated adducts [39,40]. The latter are related to the addition of different amines among which there are species involving core-anchoring groups in the synthesis of C_{60} -based star-like polymers. Lack of the experimental structural data prevents from making conclusion on the fitting degree. However, optical spectroscopy data are in full agreement with predicted behavior of the computed adducts [41].

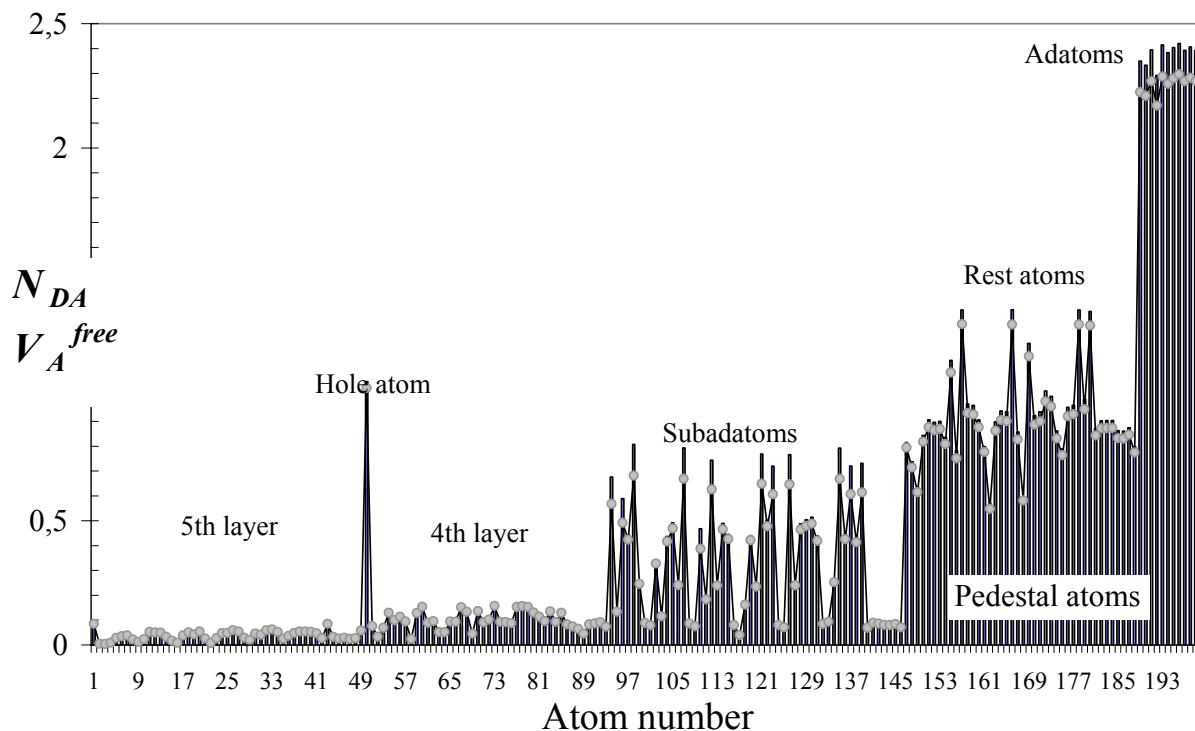


Figure 12. N_{DA} (bars) and V_A^{free} (dotted curve) maps of the Si(111)(7×7) surface unit cell.

5 ODD ELECTRONS IN THE SURFACE STUDY

The most explicitly, the approach is vivid in the case of covalent crystal surfaces. Atoms, which form the crystals, (C, Si, Ge etc.) are described by a fixed coordination number that preserves the rigid composition of the electronic configuration, practically identical for both bulk and surface. This very rigidity provided the appearance of the term “*dangling bonds*”, which has been a phenomenological characteristic mark of the surfaces until now. Let us consider the subject from the general concept of the EUPes described in the previous sections exemplifying the approach by the most actively studied Si(111)(7×7) and Si(100)(2×1) surfaces.

5.1 Si(111)(7×7) Surface

Figure 12 presents the N_{DA} map of the surface unit cell which covers 200 atoms forming 5-layer rhombic structure. As conventionally accepted (see [42] and references therein), the unit cell is characterized by 19 dangling bonds, separated between 12 adatoms, 6 rest atoms and 1 hole [43]. However, this presentation is far from reality. Calculations show that the EUPes total number N_D of the surface unit cell constitutes 92.6. The electrons are distributed over the cell atoms with density N_{DA} , shown in the figure by bars. Dotted curve in the figure presents the atom free valence calculated according to (15). As in the fullerene case, there is practically full coincidence between the N_{DA} and V_A^{free} values so that the N_{DA} map presents the chemical portrait of the surface.

Extremely high chemical activity concerning practically all atoms should be emphasized. The supreme chemical activity of the topmost atoms involving adatoms, rest atoms and holes is well proven by a variety of adsorption processes studied on the surface [42]. Important that the suggested picture explains as well the high reactivity of pedestal atoms and subadatoms which was experimentally observed when studying the surface oxidation [44,45] and which has not got any explanation until now.

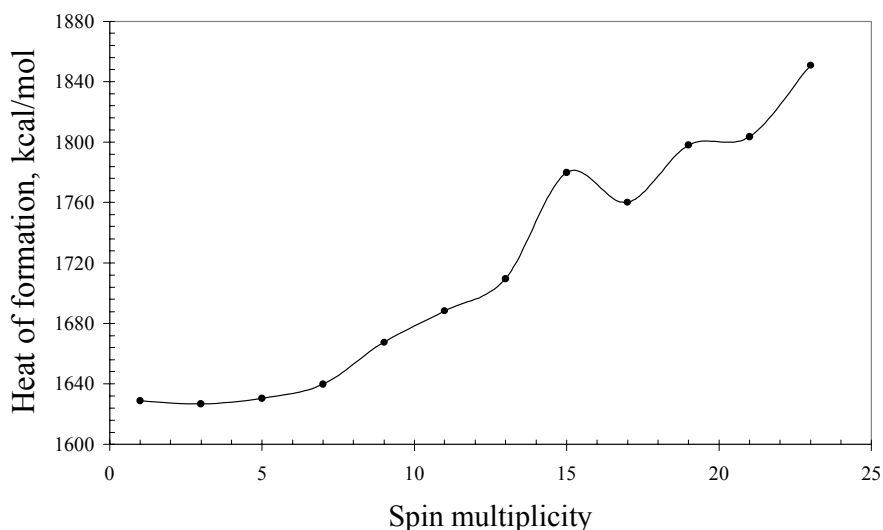


Figure 13. Energy of the high-spin states of the Si(111)(7×7) surface [48].

The surface was studied in the *embedded cell* approximation [46] when the unit cell is a part of a larger host cluster. The host cluster involves additional 42 silicon atoms and 128 hydrogenic terminators forming an outer envelop of the unit cell [47]. The total number of effectively unpaired electrons N_D of the cluster constitutes 96.6. The envelop atoms (mainly one hole and a few atoms in the 2nd and 3rd rows) contributes to the number only 4 electrons (or 4.3%) which can effect the unpaired electron behavior only slightly. Therefore, the cluster energy dependence on the spin multiplicity, low part of which is presented in Figure 13, shows the tendency characteristic for the embedded cell as well. All states shown in the figure are spin-mixed. However, the dependence clearly exhibits antiferromagnetic exchange interaction between the unpaired electrons. The exchange integral J value, determined according to (1), is -0.44 kcal/mol not depending on the S_{\max} value of either 48 or 49. The small J value is responsible for practically constant energy of the spin lowest states (with the triplet state as lowest) in the figure. However, the pure spin singlet state is the lowest by energy so that the unit ground state is singlet. At the same time the smallness of J integral is a promising factor for the surface magnetic behavior via one of mechanisms (such as van Fleck polarization [49]) promoting the magnetism of substances with the singlet ground state [50]. A peculiar distribution of the surface spin density [48] favors a multi-mode appearance of the surface magnetism that was observed experimentally [51,52].

5.2 Si(001)(2×1) Surface

From the EUPE concept the surface looks quite differently comparing with the preceding one. Due to much smaller size of the surface unit cell, there is a possibility to consider a set of the units embedded into a host cluster [46]. The total number of unpaired electrons related to the surface unit cell equals to 2.82. Figure 14 shows their distribution by the N_{DA} and V_A^{free} maps related to the assemblage of 4 unit cells of the Si(001)(2×1) surface. As previously, the maps are fully identical. According to both maps, the chemical activity of the surface oppositely to the considered above is much less by both the absolute value and the depth of penetration into the surface. Exchange interaction between the EUPEs is antiferromagnetic and much stronger. The exchange integral J , determined according to (1), constitutes -4.6 kcal/mol ($S_{\max} = 6$) that is bigger by order of magnitude than that of the Si(111)(7×7) surface. As a result, the surface should be predominantly diamagnetic with less pronounced peculiarities of magnetic behavior in comparison with the previous one.

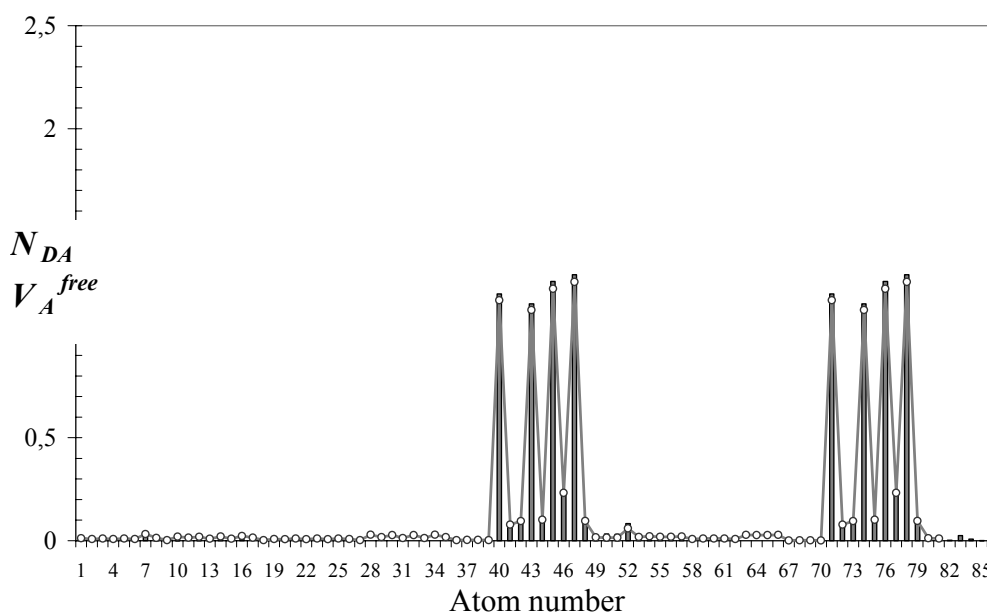


Figure 14. N_{DA} (bars) and V_A^{free} (dotted curve) maps of 8 unit cells of the Si(001)(2×1) surface.

6 MOLECULAR NANOMAGNETS

The applicability of the basic grounds related to the EUPEs considered above can be illustrated by two binuclear isostructured magnetic molecules $\text{Co}_2(\mu\text{-OH}_2)(\text{OCCMe}_3)_4(\text{HOCCMe}_3)_4$ (Co_2 -molecule) and $\text{Ni}_2(\mu\text{-OH}_2)(\text{OCCMe}_3)_4(\text{HOCCMe}_3)_4$ (Ni_2 -molecule) [53] shown in Figure 15. Electronic configurations of Co and Ni atoms are $[\text{Ar}]3d^74s^2$ and $[\text{Ar}]3d^84s^2$, respectively, so that the above molecules are traditionally characterized by 6 and 4 magnetic, or odd, electrons, correspondingly.



Figure 15. Co_2^- (left) and Ni_2^- (right) molecules. X-ray-based structures [54].

The first striking result concerns Co_2^- -molecule. As occurred, for the complex $N_D = 1$ instead of 6. The finding evidences that magnetic electrons of Co atom are antiferromagnetically coupled so that the magnetism of the molecule should be weak. The related N_{DA} map is shown in Figure 16. The picture covers Co and oxygen atoms, which surround the former. Actually, the N_{DA} values at the atoms belonging to organic ligands are zero. As seen from the figure, the N_{DA} map is spread not only over Co atoms, but concerns their oxygen surrounding as well providing a visible delocalization of spins.

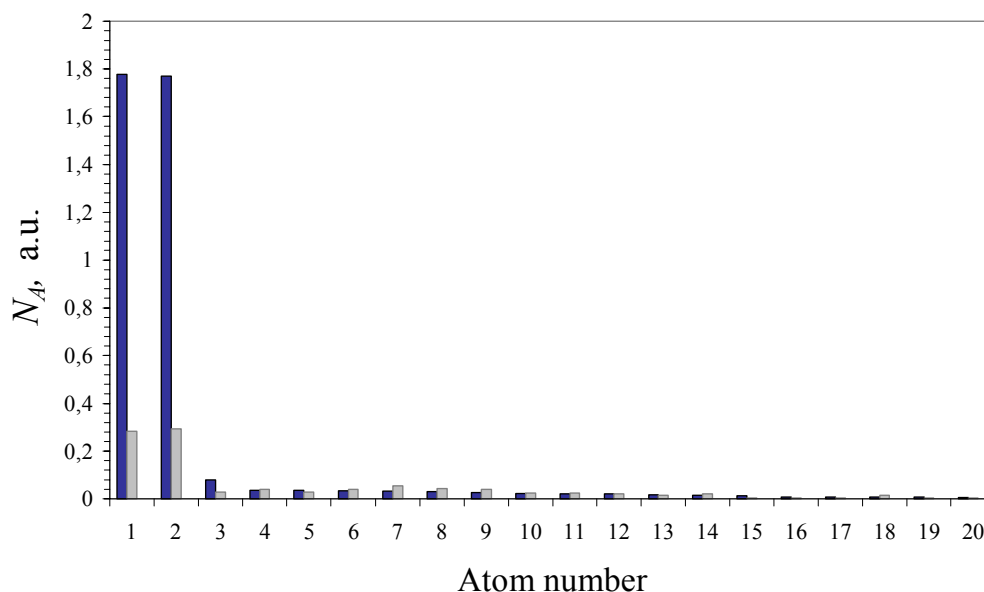


Figure 16. N_{DA} maps of the Ni_2^- (dark blue bars) and Co_2^- (light gray bars) molecules [53].

Oppositely to the Co_2^- -molecule, its Ni_2^- -counterpart behaves quite differently. The total number of the EUPEs $N_D = 4$ that does not contradict with conventional expectations. The corresponding N_{DA} map shown in Figure 16 exhibits the concentration of the largest part of unpaired electrons on Ni atoms although oxygen atoms are involved in the distribution as well thus providing spin delocalization over metal atoms and the closest surrounding. Therefore, the spin delocalization appears to be a common feature of the magnetic molecules of such type.

Different behavior of the magnetic electrons in the two molecules is well supported

experimentally. The Co_2 -molecule is weakly magnetic, showing a weak antiferromagnetism, while its Ni_2 counterpart well exhibits ferromagnetic behavior [54].

7 MAGNETISM OF POLYMERIZED C_{60}

At the end of 2001 a miracle was announced concerning a ferromagnetic behavior of polymerized C_{60} crystal [55]. The phenomenon is convincingly proved to be related to carbeneous species while its origin remains unclear until now. As usually, two governing factors are important for the phenomenon, namely, unpaired electrons as spin sources and atom and/or molecule packing. Presented in Section 5 shows that the molecule can generally serve as a spin source. At the same time is known that the molecule packing in the pristine crystal structure does not provide the magnetic behavior. Therefore one has to answer three key questions:

- 1) Does the molecules polymerization activate their magnetic ability?
- 2) Is it the molecule packing that is responsible for the magnetic behavior?
- 3) Are there some extra factors which provoke strengthening the magnetic ability?

Previous attempts to answer first two fundamental questions computationally may be reduced to the following suggestions:

- 1) Ideal polymerized crystals do not possess magnetic behavior [56].
- 2) The molecule structure that becomes active spin source providing the body magnetization if only either thermal or pressure treatment of the species under the molecule polymerization cause radical defects [57–61].
- 3) Some particular modes of molecules packing under polymerization can provoke the formation of topological defects, which become active spin sources [62–64].

Summarizing the answers leads to the conclusion on a possible defect origin of the crystal magnetism. The problem arises therewith, how enough quantity of the defects, homogeneously distributed over the crystal bulk, can be provided under the specimen production. At the same time non-stopping series of experiments on exhibition of experimental conditions which provide the phenomenon recording, have brought to a practically general conclusion that only structurally distorted crystals, of mainly rhombohedral packing show the magnetic behavior.

Let us look at the problem from the EUPE viewpoint of an individual C_{60} molecule and its polymerized assemblages. Three C_{60} oligomers corresponding to three main types of the polymer packing [55] are shown in Figure 17. Central monomeric molecules (MMs) are in the positions characteristic for macrosamples. Taking them out of the structures and calculating without changing the molecule geometry, one can obtain characteristics of the considered polymeric structures.

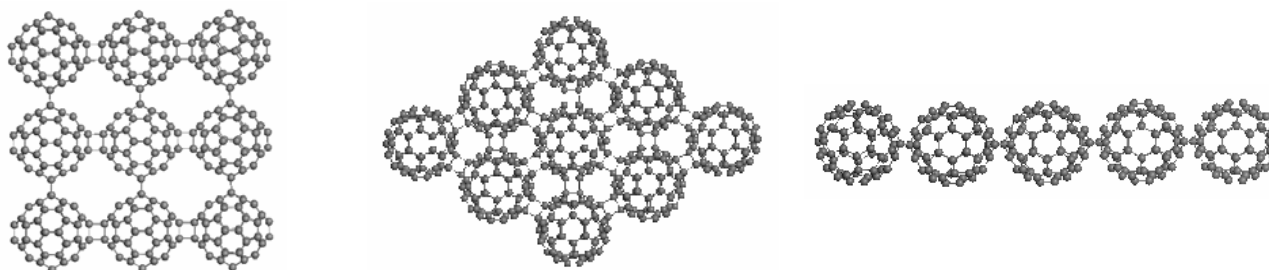


Figure 17. Equilibrated structures of the $9^*C_{60}(Hg)$, $9^*C_{60}(Tg)$, $5^*C_{60}(L)$ oligomers; UHF singlet state [65].

Table 2. UEPS Data Characteristics

Molecules & oligomers	N_D	J , kcal/mol
<i>Individual molecules</i>		
C_{60}	9.84	-1.86
C_{60} -MM(Hg)	9.41	-2.17
C_{60} -MM(Tg)	11.50	-2.10
C_{60} -MM(L)	12.04	-2.10
<i>Oligomers</i>		
$9^*C_{60}(Hg)$	9.23	-0.21
$9^*C_{60}(Tg)$	13.41	-0.23
$5^*C_{60}(L)$	12.02	-0.38

The relevant characteristics are given in Table 2. As seen from the table, the polymerization causes a significant changing in the electronic structure of the individual molecules. A considerable growth of the N_D value is observed that means a weakening of covalent pairing of odd electrons in the MM's under polymerization. However, the exchange interaction between them becomes obviously stronger so that the polymerization itself does not favor the sample magnetism. When looking at the characteristics for the whole oligomers, it should be pointed out that their exchange integrals significantly decrease by factor $\sim 1/k$, where k is the MM's number. This evidences weakening the odd electrons interaction within the whole oligomer that is quite favorable for magnetism. Thus, oligomers with a few tens of MM's may exhibit magnetic behavior. Therefore, nanostructured polymeric samples may be expected to be magnetic. This is really observed experimentally at photogenerated linear oligomerization of the C_{60} molecules in the pristine crystal body with average k about 20 [66]. Nanostructuring seems to be responsible for magnetism of the carpet-like structures as well. Thus, Rh-magnetism is the best observed for samples, which are produced at high temperature and pressure close to the limit parameters of crystal destruction [67]. It occurred possible to form a whole family of magnetic carbons with varying degree of ferromagnetic content (and/or nanostructuring). Rh-magnetic samples have high mosaicity [68] and non-uniform magnetic structure, which constitutes not more than 30% of the sample [69]. No such features, as well as no magnetism have been observed for Tg crystals [70]. Therefore nanostructuring of carbon materials with potentially unpaired electrons can be a reasonable explanation of the phenomenon.

A scale-like model for the Rh-magnetism can be suggested. Obviously, graphite-like structure

of the crystal favors “scaly” nanoclustering of the body under severe conditions [67–69]. The number and size of the scales undoubtedly depend on the technological treatment. However, consisting of a few tens of MM’s, the scales are characterized by small exchange integrals. When the latter become small, primary negative due to domination of the Coulomb term, they may change sign providing the growth of the exchange interaction contribution, just changing antiferromagnetic behavior of the scale to the ferromagnetic one. Among other mechanisms responsible for the induction of the magnetic order in systems with singlet ground state, one can suggest the van Fleck polarization mentioned above [49]. Actually, lowering the integral value results in narrowing the singlet–triplet gap, equal to $2J$, so that the ground state can easily become spin–mixed when magnetic field is applied.

The nanostructuring origin of the magnetic carbons is well supported by the observation of magnetism of the nanostructured graphite produced by the proton beam irradiation [71], of local ferromagnetism in microporous carbon with the structural regularity of zeolite Y [72], as well as of unconventional magnetism in all–carbon nanofoams [73].

Acknowledgment

The author is greatly indebted to V. A. Zayets for contributing to the CLUSTER–Z2 program codes making them sufficient for a thorough investigation of effectively unpaired electrons. The work was financially supported by the Russian Foundation for Basic Research (projects no. 03–07–90197 and 04–03–33182) and by the Federal Program “Research and Developments of Priority Trends in Science and Engineering“ in 2002–2006 (project no. ИИ–12.1/008).

8 REFERENCES

- [1] K. Takatsuka, T. Fueno, and K. Yamaguchi, *Theor. Chim. Acta.* **1978**, 48, 175–184.
- [2] L. Noodleman, *J Chem Phys.* **1981**, 74, 5737–5743.
- [3] V. N. Staroverov and E. R. Davidson, *Chem. Phys. Lett.* **2000**, 330, 161–168.
- [4] E. F. Sheka and V. A. Zayets, *Russ. Phys. Chem.* **2005**, 79, 2009–2015.
- [5] L. Salem and C. Rowland, *Angew. Chem. Intern Edit.* **1972**, 11, 92–111.
- [6] R. Hoffman, *Accounts Chem. Res.* **1971**, 4, 1–9.
- [7] J. W. Harrison, *Carbene Chemistry*, W.Kirsme (Ed.), 2nd edn., Academic Press, New York 1971, pp.159–194.
- [8] E. F. Sheka, in *Lecture Notes in Computer Science, Computational Science – ICCS2003*, Eds. P.M.A.Sloot, D.Abramson, A.V.Bogdanov, J.Dongarra, A.Y.Zomaya, and Y.E.Gorbachev, Springer: Berlin. 2003. Part II. pp.386–398.
- [9] E. F. Sheka, *Centr. Europ. Journ. Phys.* **2004**, 2, 160–182.
- [10] E. F. Sheka, *Int. Journ. Quant. Chem.* **2004**, 100, 375–387.
- [11] N. V. Kamanina and E. F. Sheka, *Optics Spectr.* **2004**, 96, 659–673.
- [12] A. W. Overhauser, *Phys. Rev. Letts.* **1960**, 4, 415–421, 466–474.
- [13] D. J. Thouless, *The Quantum Mechanics of Many–Body Systems*. AP: NY, 1961.
- [14] W. H. Adams, *Phys. Rev.* **1962**, 127, 1650–1659.
- [15] P. O. Löwdin, *Phys. Rev.* **1955**, 97, 1509–1519.
- [16] J. Koutecki, *J. Chem. Phys.* **1967**, 46, 2443–2451.
- [17] J. Čížek and J. Paldus, *J. Chem. Phys.* **1967**, 47, 3976–3985.
- [18] M. Benard, *J. Chem. Phys.* **1979**, 71, 2546–2556.
- [19] P. J. Hay, J. C. Thibault, and R. Hoffman, *JACS* **1975**, 97, 4884–4899.
- [20] D. A. Zhogolev and V. B. Volkov, *Methods, Algorithms and Programs for Quantum–Chemical Calculations of Molecules* (in Russian), Naukova Dumka: Kiev .1976.
- [21] V. A. Zayets, *CLUSTER–Z1: Quantum–Chemical Software for Calculations in the s,p–Basis*”, Institute of Surface Chemistry, Nat. Ac.Sci. of Ukraine: Kiev, 1990.

- [22] E. F. Sheka and L. A. Chernozatonskii (to be published).
- [23] K. Hedberg, L. Hedberg, D. S. Bethune, C. A. Brown, M. de Vries, H. C. Dorn, and R. D. Johnson, *Science* **1991**, *254*, 410–414.
- [24] L. Hedberg, K. Hedberg, O. V. Boltalina, N. A. Galeva, A. S. Zapolskii, and V. F. Bagryantsev, *J. Phys. Chem.* **2004**, *108*, 4731–4736.
- [25] F. Leclercq, P. Damay, M. Foukani, P. Chieux, M. C. Bellisent-Funnel, A. Rassat, and C. Fabre, *Phys. Rev.* **1993**, *48B*, 2748–2753.
- [26] Yu. L. Slovokhotov, I. V. Moskaleva, V. I. Shil'nikov, E. F. Valeev, Yu. N. Novikov, A. I. Yanovski, and Yu. T. Struchkov, *Mol. Mat.* **1996**, *8*, 117–122.
- [27] G. Orlandi and F. Negri, *Photochem. Photobiol. Sci.* **2002**, *1*, 289–308.
- [28] P. J. Horoyski, M. L. W. Thewalt, and T. R. Anthony, *Phys. Rev.* **1996**, *54B*, 920–928.
- [29] K. B. Wiberg, *Tetrahedron.* **1968**, *24*, 1083–1086.
- [30] S. G. Semenov, in *Evolution of the Valence Doctrine* (in Russian), Moscow, Khimia. 1977. pp.148–154.
- [31] B. M. Bulychev, and I. A. Udod, *Mendeleev Commun.* **1995**, *39*, 9–14.
- [32] N. I. Alekseev and G. A. Dyuzhev, *Zhurn. Tekhn. Fiz.* **2001**, *46*, 573–578.
- [33] E. F. Sheka. *Zhurn. Strukt. Khimii* (Russ. Struct. Chem.) **2006**, *47*, 613–619.
- [34] O. V. Boltalina and N. A. Galeva. *Uspekhi khimii* **2000**, *69*, 661–682.
- [35] L. N. Sidorov and O. V. Boltalina. *Uspekhi khimii* **2002**, *71*, 611–632.
- [36] E. F. Sheka (to be published).
- [37] I. S. Neretin, K. A. Lyssenko, M. Yu. Antipin, Yu. L. Slovokhotov, O. V. Boltalina, P. A. Troshin, A. Yu. Lukonin, L. N. Sidorov, and R. Taylor, *Angew. Chem.* **2000**, *112*, 3411–3416.
- [38] A. Papoular, **2005** (private communication).
- [39] E. F. Sheka, *Book of Abstracts of the 8th Fock School on Quantum Chemistry* (V.Novgorod, 26–30 April, 2004). 2004, P977.
- [40] N. P. Yevlampieva, and E. F. Sheka, *Fullerenes, Nanotubes and Carbon Nanostructures* (in press).
- [41] E. F. Sheka, B. S. Razbirin, A. N. Starukhin, and K. S. Nelson. *Optics Spectr.* (in press).
- [42] Zh. He, Q. Li, and K. T. Leng, *J. Phys. Chem.* **2005**, *109B*, 14908–14913.
- [43] K. Takayanagi, Y. Tanishiro, M. Takahashi, and S. Takahashi, *Surf. Sci.* **1985**, *164*, 367–375.
- [44] J. J. Boland and J. S. Vallarubia, *Science* **1990**, *248*, 838–841.
- [45] H. Ibach, H. D. Bruchmann, and H. Wagner, *Appl. Phys.* **1982**, *29A*, 113.
- [46] E. A. Nikitina, E. F. Sheka, and M. Aono, *Phys. Low-Dim. Struct.* **2001**, *1/2*, 31–56.
- [47] V. Khavryutchenko, E. Sheka, D. H. Huang, and M. Aono, *Phys. Low-Dim. Struct.* **1998**, *3/4*, 81–106.
- [48] E. F. Sheka, E. A. Nikitina, and V. A. Zayatz, *Surf. Sci.* **2003**, *532–535*, 754–756.
- [49] J. H. van Fleck, *The Theory of Electric and Magnetic Susceptibilities*. Oxford. 1932.
- [50] A. K. Zvezdin, V. M. Matveev, A. A. Mukhin, and A. I. Popov, *Rare Earth Ions in Magnetoordered Crystals* (in Russian). Nauka: Moscow. 1985. Chapter 10. pp.167–182.
- [51] Z. Wu, T. Nakayama, M. Sakurai, and M. Aono. *First International Symposium on Nanoarchitectonics Using Suprainteraction – NASI-1*, 2000 (Tsukuba, Japan, 13–15 November 2000).
- [52] V. Venkataraman, K. Nogushi, M. Aono, and T. Suzuki. *Appl. Phys. B* **2002** DOI: 10.1007/s003400200848.
- [53] E. F. Sheka in *1st Iran–Russia Joint Seminar & Workshop on Nanotechnology*. Aftab Graphic: Teheran. **2005**, pp.31–44.
- [54] T. B. Mikajlova, E. V. Pakhmutova, A. E. Malkov, I. F. Golovaneva, A. A. Sidorov, I. G. Fomina, G. G. Aleksandrov, V. N. Ikorskii, V. M. Novotorzev, I. L. Eremenko, and I. I. Moiseev, *Izv. Akad. Nauk Rossii, ser. khim.* **2005**.
- [55] T. L. Makarova, B. Sundquist, R. Hohne, P. Esquinazi, Ya. Kopelevich, P. Scharff, V. A. Davydov, L. S. Kashevarova, and A. V. Rakhmanina, *Nature*, **2001**, *413*, 716–718.
- [56] S. Okada and A. Osiyama, *Phys. Rev.* **2003**, *B 68*, 235402–1–5.
- [57] A. N. Andriotis, M. Menon, R. M. Sheetz, and L. Chernozatonskii, *Phys. Rev. Lett.* **2003**, *90*, 026801–1–4.
- [58] J. Ribos–Ariño and J. J. Novoa, *J. Phys. Chem. Sol.* **2004**, *65*, 787–791.
- [59] J. Ribos–Ariño, and J. J. Novoa, *Angew. Chem. Int.* **2004**, *43*, 577–580.
- [60] V. V. Belavin, L. G. Bulusheva, A. V. Okotrub, and T. L. Makarova, *Phys. Rev.* **2004**, *70B*, 15402–15409.
- [61] P. O. Lehtinen, A. S. Foster, A. Ayuela, A. Krashennnikov, K. Norlund, and R. M. Niemen, *Phys. Rev. Lett.* **2003**, *91*, 017202–1–4.
- [62] N. Park, M. Yoon, S. Berber, J. Ihm, E. Osawa, and D. Tománek, *Phys. Rev. Lett.* **2003**, *91*, 237204–1–4.
- [63] K. Wakabayashi and K. Harigaya, *J. Phys. Soc. Jap.* **2003**, *72*, 998–1002.
- [64] Y. –H. Kim, J. Choi, J. Chang, and D. Tománek, *Phys. Rev.* **2003**, *68B*, 125420–1–4.
- [65] E. F. Sheka, V. A. Zayets, and I. Ya. Ginzburg, *Zhurn. Eksp. Teoret. Fiziki* (in press).
- [66] F. J. Owens, Z. Iqbal, L. Belova, and K. V. Rao, *Phys. Rev.* **2004**, *69B*, 033403–1–3.
- [67] R. A. Wood, M. H. Lewis, M. R. Lees, S. M. Bennington, M. G. Cain, and N. Kitamura, *J. Phys. Condens.*

Matter. **2002**, *14*, L385–388.

- [68] M. Tokumoto, B. Narymbetov, H. Kobayashi, T. L.M akarova, V. A. Davydov, A. V. Rakhmanina, and L. S. Kashevarova, in *Electronic Properties of Novel Materials – Molecular Nanostructures*. Eds. H.Kuzmani, J.Fink, M. Mehrang, S. Roth. AIP Conf. Proc. 544 (AIP, Melville, New York, 2000) **2000**, pp.73–77.
- [69] K. –H. Han, D. Speman, R. Hohne, A. Setzer, T. Makarova, P. Esquinazi, and T. Butz, *Carbon* **2003**, *41*, 785–795.
- [70] V. A. Davydov, V. Agafonov, H. Allouchi, R. Ceolin, A. V. Dzyabchenko, and H. Szwarc, *Synthet. Met.* **1999**, *103*, 2415–2420.
- [71] P. Esquinazi, D. Speman, R. Hohne, A. Setzer, K. –H. Han, and T. Butz, *Phys. Rev. Lett.* **2003**, *91*, 227201–1–3.
- [72] Y. Kopelevich, R. R. da Silva, J. H. S. Torres, A. Penicaud, and T. Kyotani, *Phys. Rev.* **2003**, *68B*, 92408–1–4.
- [73] A. V. Rode, E. G. Gamaly, A. G. Christy, J. G. E. Gerald, S. T. Hyde, R. G. Elliman, B. Luther–Davies, A. I. Veinger, J. Androulakis, and J. Giapintzakis, *Phys.Rev.* **2004**, *70B*, 054407–1–9.

Biographies

Prof. Elena F.Sheka graduated from the Kiev State University on physics and spectroscopy. She was with the Institute of Physics of the Academy of Sciences of the Ukrainian SSR (Kiev) 1958–1966; the Institute of Solid State Physics of the Ac.Sci of the USSR (Chernogolovka, Mosc. distr.) 1966–1986; the Moscow Physical–Technical Institute (professorship) 1978–1986; and the Russian Peoples’ Friendship University (RPFU) (Moscow) since 1986 till now. She takes the position of a principal scientist of the Research Department of the RPFU. Prof. E. F. Sheka is the author of more than 240 papers and two monographs. She is a member of the editorial board of *Molecular Crystals and Liquid Crystals* (Gordon and Breach Publ.); an associate editor of the *Journal of Nanoparticle Research* (Springer); a full member of the European Society of Computational Methods in Science and Engineering (ESCMSE). Her fields of interests cover excitonics of molecular crystals, phonon spectra of molecular crystals (inelastic neutron scattering mainly), exciton–phonon interaction and vibronic spectra of molecular crystals, phase transformation in molecular solids with liquid–crystal behavior (vibrational spectroscopy and neutron diffraction), vibrational spectroscopy of nanoparticles, quantum–chemical simulations of nanoobjects towards computational nanotechnology, quantum fullerenics.